Heliyon 7 (2021) e06047

Contents lists available at ScienceDirect

Heliyon

journal homepage: www.cell.com/heliyon

Research article

Application of artificial neural network modeling techniques to signal strength computation

K.C. Igwe [a,*], O.D. Oyedum [a], A.M. Aibinu [b], M.O. Ajewole [c], A.S. Moses [a]

[a] Department of Physics, Federal University of Technology, P.M.B. 65, Minna, Niger State, Nigeria
[b] Department of Mechatronics Engineering, Federal University of Technology, P.M.B. 65, Minna, Niger State, Nigeria
[c] Department of Physics, Federal University of Technology, P.M.B. 704, Akure, Ondo State, Nigeria

ARTICLE INFO

Keywords:
Artificial neural network
Atmospheric parameters
Received signal strength
Very high frequency

ABSTRACT

This paper presents development of artificial neural network (ANN) models to compute received signal strength (RSS) for four VHF (very high frequency) broadcast stations using measured atmospheric parameters. The network was trained using Levenberg-Marquardt back-propagation (LMBP) algorithm. Evaluation of different effects of activation functions at the hidden and output layers, variation of number of neurons in the hidden layer and the use of different types of data normalisation were systematically applied in the training process. The mean and variance of calculated MSE (mean square error) for ten different iterations were compared for each network. From the results, the ANN model performed reasonably well as computed signal strength values had a good fit with the measured values. The computed MSE were very low with values ranging between 0.0027 and 0.0043. The accuracy of the trained model was tested on different datasets and it yielded good results with MSE of 0.0069 for one dataset and 0.0040 for another dataset. The measured field strength was also compared with ANN and ITU-R P. 526 diffraction models and a strong correlation was found to exist between the measured field strength and ANN computed signals, but no correlation existed between the measured field strength and the predicted field strength from diffraction model. ANN has thus proved to be a useful tool in computing signal strength based on atmospheric parameters.

1. Introduction

In order to obtain the desired communication between a transmitter and a receiver, knowledge of the variability of field strength in the link is needed. This is significant in applications that require high quality signals such as broadcast networks [1]. Also, the emerging and advanced development of radio communication systems today has necessitated careful planning and design of the links [2, 3].

A number of mechanisms that affect signal propagation are usually considered when planning for VHF/UHF broadcast services. Some of these include free space attenuation, diffraction over obstacles, tropospheric scatter, reflection from the earth's surface and refraction in the earth's atmosphere [4]. The propagating medium between a transmitter and a receiver is a serious determining factor on the performance of wireless radio communication systems. This is due to the random nature of a wireless radio channel since it depends on atmospheric variables like temperature, pressure, humidity, hydrometeors and atmospheric gases [5].

The estimation of field strength at VHF and UHF bands is a function of the effects of the refractive nature of the atmosphere and the location of the transmitter and receiver [6]. The differences between the actual and estimated values of field strength may be a consequence of the variations in atmospheric conditions. Such variations can impact the field strength positively or negatively for a substantial period. Long-term changes may arise when the variation of the atmospheric radio refractive index gradient is pronounced from the normal propagation values [4]. It is therefore pertinent to understand the effects of weather on radio wave propagation in order to improve the quality of radio communication signals [7, 8, 9]. Consequently, radio propagation models provide efficient methods of analysing and predicting the strength of these signals in this regard [10].

Different types of models have been employed by the International Telecommunication Union-Radio (ITU-R) for the prediction of field strength when planning for point-to-area (broadcast) services, albeit with some limitations. For services with frequencies from 30 MHz to 1000 MHz, procedures provided by Recommendation P. 370-7 [11] are

* Corresponding author.
E-mail address: k.igwe@futminna.edu.ng (K.C. Igwe).

https://doi.org/10.1016/j.heliyon.2021.e06047
Received 8 June 2020; Received in revised form 23 September 2020; Accepted 18 January 2021

subjected to some conditions: The measured field strengths are adjusted to correspond to a power of 1 kW radiated from a half-wave pole. Also, the derived curves are based on data measured in temperate climates, thereby restricting its universal usage. Recommendation P.528-3 [12] was adopted as a guide for the prediction of path loss for the aeronautical mobile services using the frequency range of 125 MHz to 30 GHz, with a distance range of up to 1800 km but the curves generated were based on data obtained mainly for a continental temperate climate. So, caution was given for its usage in other climates.

In order to calculate received field strengths over diffraction paths, Recommendation P.526-12 [13] was derived by providing several models that are applicable to different types of obstacles and to different path geometries, but this recommendation uses only antenna heights and range between the transmitter and the receiver to predict path losses. Another very popular ITU-R model is the Recommendation P. 1546-5 [14] which provides a method of field strength predictions for terrestrial services for the broadcast, land mobile, maritime mobile and certain fixed services operating between 30 MHz and 3000 MHz and at the distance range of 1 km–1000 km. This model uses interpolation and extrapolation of transmitting and receiving antenna heights and the distance between them, operating frequency, relevant percentage of time, terrain clearance angle and others. Like the other Recommendations, the ITU-R P.1546-5 did not take cognisance of the intervening atmospheric conditions between the transmitter and receiver. This important oversight is the main focus of this effort.

The approach presented in this paper uses artificial neural network model to compute the received signal strength for VHF-FM and TV point-to-area services from weather parameters. This method is based on the knowledge of the signal propagation mechanisms earlier mentioned. Also, the importance of finding accurate propagation characteristics for different localities, particularly in the tropics, as encouraged by ITU-R has necessitated the acquisition of weather data, since they are relatively cheaper and readily available compared to the high cost of procuring signal strength measuring equipment.

The neural network training is based on measurements of some weather variables: temperature, pressure, humidity and wind speed. This paper is a continuation and extension of an earlier version [15]. In this paper, we propose an increase of the number of hidden layer neurons to 20 and the number of normalisation types to 4.

The rest of the paper is organised as follows: Section 2 provides the background comprising of an overview of artificial neural network, while section 3 presents the materials and methods including the model design and development. Section 4 presents the results and discussion, while section 5 presents the conclusion.

2. Background

It has been established by several authors that radio refractivity correlates with radio signal strength [7, 16, 17, 18]. By inference, the atmospheric variables (temperature, pressure, relative humidity) from which radio refractivity derives have also been found to correlate with radio signal strength and this has been reported by a number of researchers. Some studies have reported the existence of correlation between RSS and atmospheric parameters of humidity and temperature [7, 19, 20, 21], while others have found correlation between RSS and wind speed [22, 23, 24, 25, 26].

It is on this basis that these atmospheric variables were used as input data to the ANN for the computation of the RSS.

2.1. Overview of artificial neural network

The artificial neural network is patterned after the human biological neural system prototype. It consists of numerous interrelated simple processing elements called neurons. These neurons receive input signals from the environment. The signals are transformed by connecting weights and through a process of training, the neurons get activated by transfer functions to give a desired output [27, 28].

ANN, which is a computational intelligence technique has been successfully used for forecasting and has been found to be more efficient than the standard empirical models. Neural networks have been very effective for modeling and for characterisation of complex systems for a number of applications [29, 30]. The successful application of ANN to a number of scientific and engineering problems abounds [31, 32, 33, 34, 35], including the prediction of signal strength in the VHF and UHF bands [2, 36, 37, 38, 39, 40, 41].

One of the most widely used type of ANN is the feedforward network. The architecture of a feedforward neural network is nonlinear whereby the output is obtained from the input through a feedforward arrangement. The multi-layer perceptron (MLP) is a type of feedforward neural network, consisting of input, hidden and output layers. The MLP uses the back-propagation (BP) learning technique [42, 43, 44].

2.1.1. Activation/transfer function

The activation (or transfer) function, $f(x)$, is responsible for the connection between the input and the output of a node and a network. The following are types of activation functions:

(i) Purelin or Linear activation function, written mathematically as

$$f(x) = x \tag{1}$$

(ii) Tansig activation function, given as

$$f(x) = \frac{2}{1 + e^{-2x}} - 1 \tag{2}$$

(iii) Logsig activation function, expressed as

$$f(x) = \frac{1}{1 + e^{-x}} \tag{3}$$

2.1.2. Normalisation

Normalisation is a data scaling technique normally applied to the neural network during training. This method standardises the values of all the input variables. The output of a neural network is greatly improved when the appropriate standardisation techniques are applied. Some types of normalisation techniques are:

(i) Min Max normalisation: Carries out a linear transformation on the original data. It normalises the data in the range 0 to +1 using the formula:

$$x_n = \frac{x - x_{min}}{x_{max} - x_{min}} \tag{4}$$

where:

x = data value to be normalised,
x_n = normalised value of x
x_{min} = minimum value of x
x_{max} = maximum value of x

(ii) Z-Score normalisation, also called zero-mean normalisation, uses the mean $\overline{x}$ and standard deviation σ for each variable across a set of training data to normalise each input variable vector.

It is expressed as:

$$Z_{score} = \frac{(x - \overline{x})}{\sigma} \tag{5}$$

(iii) Unitary data normalisation is a simple type of normalisation that is expressed as:

$$x_n = \frac{x}{x_{max}} \tag{6}$$

(iv) Decimal Scaling normalisation standardises the given data by moving the decimal points of values of feature A. A value x of A is normalised to x_n by the following expression:

$$x_n = \frac{x}{10^m} \tag{7}$$

where:

A = values of the measured data set
m = the smallest integer such that $\max|x_n| < 1$

3. Materials and methods

The measurement of the received signal strength was carried out from four broadcast transmitters situated in different parts of Niger State, Central Nigeria. The VHF stations are the Nigerian Television Authority (NTA) Minna transmitting at a frequency of 210.25 MHz, Search FM transmitting at 92.3 MHz, Crystal FM transmitting at 91.2 MHz and Power FM transmitting at 100.5 MHz. The measurement site is the laboratory building of Physics Department, Federal University of Technology, Minna (FUTMinna), Niger State. Six months of data measurements were carried out: Three dry months (January–March) and three wet months (May–July). The measurement parameters for the links are given in Table 1, while maps of the transmitting stations and the measurement site are shown in Figures 1 and 2.

The signal strength was measured using Geberit digital signal level meter, GE-5499. The signal level meter covers a frequency range of 45–860 MHz, bandwidth $>$ 300 kHz and a signal strength range of 30–120 dBμV. It has a resolution of 0.1 dBμV and a level of accuracy of ±1. A dipole antenna was connected to the signal level meter to enable a good signal reception. The digital signal level meter and antenna are shown in Figure 3.

The weather data (pressure, temperature, relative humidity and wind speed) used in this work were measured at the Tropospheric Data Acquisition Network (TRODAN) located at the mini campus of FUT-Minna. The Campbell CR-1000 data logger was employed for this measurement. The CR-1000 is powered by a 12 V DC source. A lithium battery backs up its clock, program and memory in case of power loss. Attached to the data logger are sensors that measure these weather parameters. These sensors accurately and precisely transduce environmental changes into measurable electrical properties by outputting voltages, changing resistances, pulses or changing states. The CR-1000 is capable of measuring any sensor with an electrical response. It measures electrical signals and converts the values to digital units, performs calculations and reduces data to statistical digital values; it also logs the measured data in its memory awaiting transfer to a PC. The Campbell CR-1000 is shown in Figure 4.

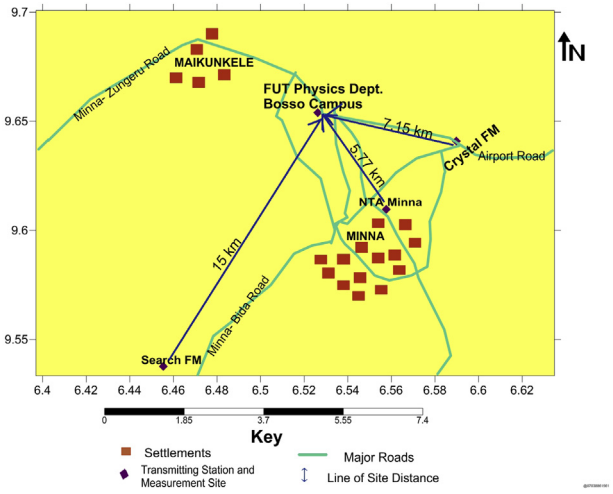

Figure 1. Transmitting stations and measurement site.

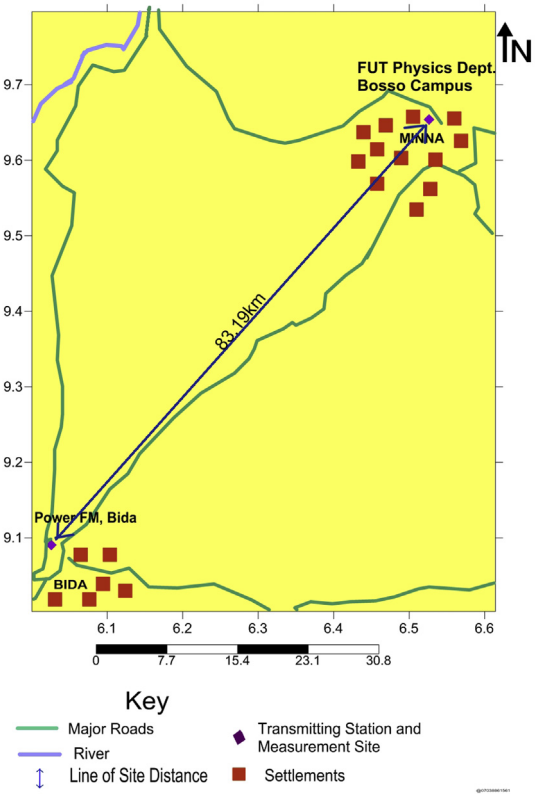

Figure 2. Distant transmitting station and measurement site.

Table 1. Parameters of the VHF links.

Frequency (MHz)	210.25	92.3	91.2	100.5
Tx height (m)	150.00	180.00	450.00	540.00
Rx height (m)	3.20	3.20	3.20	3.20
Path distance (km)	5.77	15.00	7.15	83.19
Tx Power (kW)	10.00	0.30	15.00	8.50

Tx = Transmitter, Rx = Receiver.

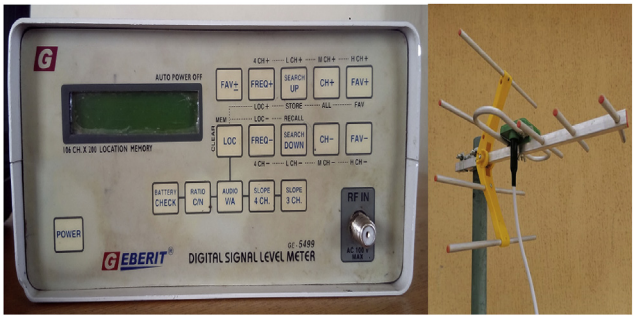

Figure 3. Geberit digital signal meter with antenna.

Figure 4. Campbell CR-1000 data logger.

3.1. Model design and development

The Levenberg-Marquardt (LM) back-propagation algorithm was used for training the network. The LM is a type of feedforward back-propagation algorithm. The data fed into the ANN as input are measured values of temperature, pressure, relative humidity and wind speed. The multilayer perceptron network proposed is shown in Figure 5.

As shown in Figure 5, the proposed MLP network comprises of four nodes (x_i for $1 \leq i \leq 4$) at the input layer, one hidden layer and one node at the output layer. The sets of adjustable weights are represented by w_{ij} and u_{jk} where w_{ij} joins the *ith* input node to the *jth* neuron in the hidden layer, while the *jth* output in the hidden layer is connected to the *kth* node in the output layer by u_{jk}; y_k ($k = 1$ in this case) is the output layer. The neuron and the output node are each linked to adjustable bias values b_j and b_k: b_j is linked with the *jth* neuron in the first network layer (i.e. layer 1), while b_k (k = 1) is linked with the node in layer 2. The weights *w*, the summing and multiplication operators, the bias b, and the activation functions are all contained in each network layer [42].

Transforming Figure 5 mathematically, layer 1 is written as

$$y_k = \left(\sum_{i=1}^{4} w_{ij} x_i + b_j\right) \tag{8}$$

where y_k is the output layer, while *k* is the *kth* neuron in the output layer, but since $k = 1$, $y_k = y_1$.

Thus, layer 2 is written as

$$y_1 = \varphi_2\left(\sum_{j=1}^{n} u_{j1}\varphi_1\left(\sum_{i=1}^{4} w_{ij} x_i + b_j\right) + b_1\right) \tag{9}$$

where *n* is the total number of neurons in the hidden layer, y_1 is the output layer.

Consequently, for layer *N*, the network is further represented by

$$y_1 = \varphi_N\left(\sum_{i=1}^{v} w_{kl} \ldots \frac{\varphi_2\left(\sum_{j=1}^{n} u_{jk} \frac{\varphi_1\left(\sum_{i=1}^{m} w_{ij} x_i + b_j\right)}{layer1} + b_k\right)}{layer2} + \ldots + b_1\right) \Bigg/ layerN \tag{10}$$

where *v* is the maximum number of neurons in layer *N*, *l* is the number of the *l*th neuron in layer *N*, while *N* is the total number of network layers.

Using layer 2 with linear activation function in the hidden and output layers, *n* number of neurons in the hidden layer and multiplying with the corresponding layer and input weights, Eq. (9) is then rewritten as

$$y = [H * G]x_i + [H * b_1] + b_2 \tag{11}$$

$$y = H[G * x_i + b_1] + b_2 \tag{12}$$

where:

H = Layer weight = [1 x *n* double] matrix
G = Input weight = [*n* x 4 double] matrix
x_i = Input vector = [4 x 1] matrix (in this case, temperature T, pressure P, relative humidity R and wind speed W)
b_1 = Layer 1 bias = [*n* x 1 double] matrix
b_2 = Layer 2 bias = constant (c)

Therefore, if

$$[H * G] = [\partial\lambda\rho\tau] \tag{13}$$

then

$$[H * G]x_i = [\partial\ \lambda\ \rho\ \tau] * [4\ \text{x}\ 1] = [\partial\ \lambda\ \rho\ \tau] * \begin{bmatrix} T \\ P \\ R \\ W \end{bmatrix} \tag{14}$$

The proposed model equation is thus given as

$$y = \partial T + \lambda P + \rho R + \tau W + c \tag{15}$$

where $\partial, \lambda, \rho, \tau$and*c* are constant values.

Following the same procedures, if Logsig activation function is used in the hidden layer, while Linear (Purelin) activation function is used in the output layer, the proposed model equation would be given as

$$y = \frac{\partial}{1 + \exp - (\lambda x_i + b)} + c \tag{16}$$

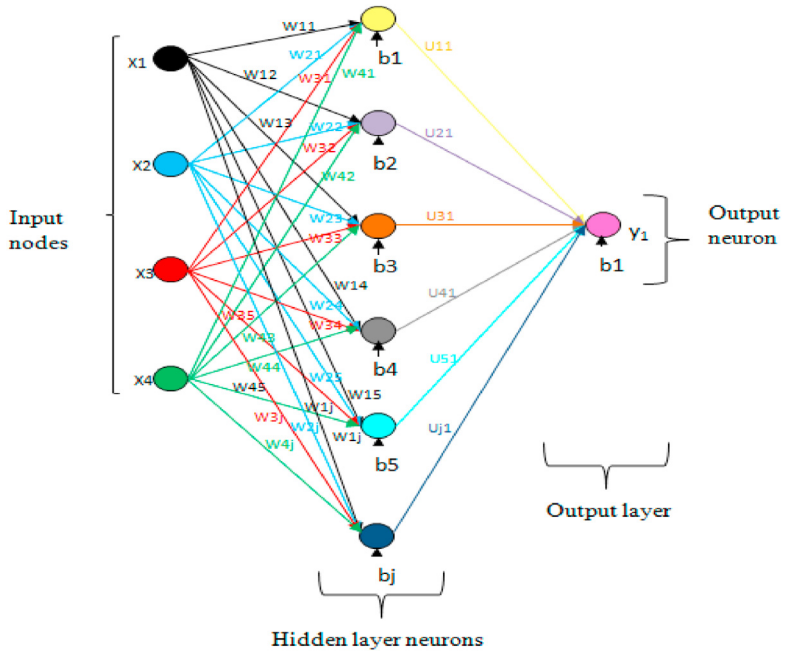

Figure 5. MLP structure of proposed model.

For Tansig activation function in the hidden layer and Linear activation function in the output layer, the model equation would be

$$y = \partial\left(\frac{2}{1+\exp -2(\lambda x_i + b)} - 1\right) + c \tag{17}$$

For Tansig activation function in the hidden layer and Logsig activation function in the output layer, the model equation would be

$$y = \frac{1}{1+\exp\left(-\left(\partial\left(\frac{2}{1+\exp(-2(\lambda x_i+b))} - 1\right) + c\right)\right)} \tag{18}$$

For Logsig activation function in the hidden layer and Tansig activation function in the output layer, the model equation would be

$$y = \frac{2}{1+\exp\left(-2\left(\partial\left(\frac{1}{1+\exp(-(\lambda x_i+b))}\right) + c\right)\right)} - 1 \tag{19}$$

For Tansig activation function in the hidden layer and Tansig activation function in the output layer, the model equation would be

$$y = \frac{2}{1+\exp\left(-2\left(\partial\left(\frac{2}{1+\exp(-(\lambda x_i+b))} - 1\right) + c\right)\right)} - 1 \tag{20}$$

For Logsig activation function in the hidden layer and Logsig activation function in the output layer, the model equation would be

$$y = \frac{1}{1+\exp\left(-\left(\partial\left(\frac{1}{1+\exp(-2(\lambda x_i+b))}\right) + c\right)\right)} \tag{21}$$

Table 2 gives the summary of the ANN training parameters.

The results of the neural network training were evaluated using the mean square error (MSE). The MSE is given as:

$$\frac{1}{N}\sum_{i=1}^{N}(y_i - x_i)^2 \tag{22}$$

where:

y_i is the predicted value
x_i is the measured value
N is the number of data points

4. Results and discussion

In the ANN training process, different parameters were evaluated. These are the effects of transfer functions at the hidden and output layers, number of hidden layer neurons and the application of different types of data normalisation. Ten different iterations were attempted and comparison was made between the mean and variance of the results.

Table 2. Summary of ANN training parameters.

Input nodes	Output nodes	Transfer function arrangement (Hidden/Output)	Data normalisation	No. of neurons
4	1	Purelin/Purelin	Min-Max	1–20
		Purelin/Logsig	Dec. Scaling	
		Purelin/Tansig	Z-Score	
		Logsig/Purelin	Unitary	
		Logsig/Logsig		
		Logsig/Tansig		
		Tansig/Purelin		
		Tansig/Logsig		
		Tansig/Tansig		

Table 3. Effect of activation functions.

Hidden Layer	Output Layer	Mean (/100)	Variance (/100)
Purelin	Purelin	1.10	0.15
Purelin	Logsig	1.10	2.50
Purelin	Tansig	1.10	1.30
Logsig	Purelin	1.10	9.70
Logsig	Logsig	1.10	0.61
Logsig	Tansig	1.10	2.60
Tansig	Purelin	0.91	1.90
Tansig	Logsig	1.10	1.10
Tansig	Tansig	1.20	0.36

The first parameter to be evaluated was the effect of transfer functions. In this process, the transfer functions in the hidden layer were varied, while the number of hidden layer neurons were held constant. Also, the transfer functions at the output layer were held constant. Thereafter, the transfer functions at the output layer were varied, while the number of hidden layer neurons and the transfer functions in the hidden layer were held constant. Using the MSE as the performance analysis measure, it was computed for the ANN model output of each network. Consequently, the network with the least MSE was selected. The results for these iterations are given in Table 3.

From Table 3, it is observed that the combination of Tansig transfer function in the hidden layer and Purelin transfer function at the output layer gave better accuracy than the other sets of transfer functions. Thus, this combination was chosen.

The second parameter investigated was the effect of number of neurons in the hidden layer. In this case, the number of neurons was varied from 1 to 20, while the already established transfer functions were held constant. This was done to test the assertion of the authors in the previous work [15] where the number of neurons was only varied from 1 to 10. The effect of number of neurons on the neural network is shown in Figure 6.

It is observed in Figure 6 that increasing the number of neurons above 9 in the hidden layer does not improve the accuracy of the model which validates the result obtained in the earlier work by the authors. Hence, the choice of neuron number 9 was made as the ideal neuron in the hidden layer.

The third parameter analysed was the application of normalisation technique. This was done to further enhance the optimal performance of the network. All the normalisation techniques outlined in subsection 2.1.2 were applied to the data. The result of the computed MSE for the four types of normalisation is presented in Table 4.

It can be observed from the MSE computed in Table 4 that Unitary normalisation yielded the overall least MSE for all the stations and thus adjudged the best type of normalisation for the proposed model as against Decimal Scaling used in the previous work.

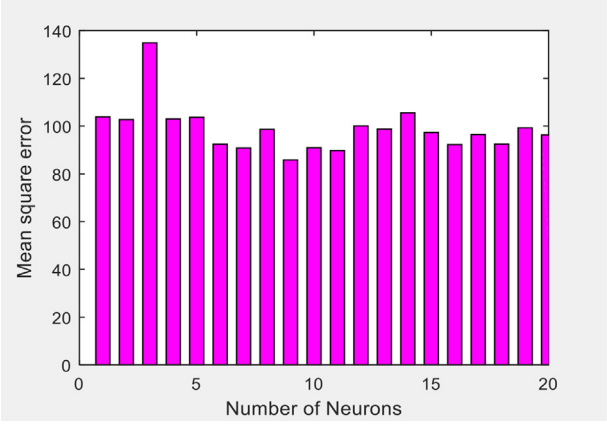

Figure 6. Effect of neuron number.

Consequent upon the foregoing findings, the proposed model was trained using Tansig transfer function and neuron number 9 in the hidden layer, Purelin transfer function in the output layer and Unitary data normalisation. The resultant effects of these parameters contributed largely to improve the general performance of the network. The training of the network was done using measured data from Crystal FM link.

On examining the accuracy and sensitivity of the network, model parameters (activation functions, neuron number and normalisation type) derived from the initial training of data obtained from Crystal FM link were used in the training between NTA and Search FM links. A total of 150 data points was used in computing the signal strength. 100 data points (≈70%) were used to train the model, while the remaining 50 data points (≈30%) were used as test data to determine the accuracy of the models. The results are given in Figures 7 and 8.

It is seen from Figures 7 and 8 that the modeled output from the ANN network performed remarkably well as computed values are close to the measured values, with minimal errors. The computed MSE values are 0.0027 and 0.0043 for the NTA and Search FM links respectively.

Model equations were derived from the trained neural networks. Eqs. (23), (24), and (25) give the derived equations from the ANN models.

The model equation from the Crystal FM link is

$$y = \partial\left(\frac{2}{1+\exp-2(\lambda x_i + b)} - 1\right) + 1.102 \tag{23}$$

model equation from the Search FM link is given as

$$y = \partial\left(\frac{2}{1+\exp-2(\lambda x_i + b)} - 1\right) + 0.777 \tag{24}$$

while the model equation from the NTA link is

$$y = \partial\left(\frac{2}{1+\exp-2(\lambda x_i + b)} - 1\right) + 1.209 \tag{25}$$

where

y = signal strength (dBμV)
x_i = input vector of temperature, pressure, relative humidity and wind speed
∂, λ *and* b are constants.

4.1. Testing of the developed model

The model developed from NTA data was tested on another dataset measured from Power FM link. The result obtained is presented in Figure 9.

From Figure 9, it can be seen that the performance of the model is good as modeled RSS values are close to the actual RSS values, with low MSE. The computed MSE from the test result is 0.0069.

Further accuracy test was carried out as the developed ANN model from Search FM data was tested on an entirely different dataset from NTA

Table 4. Effect of normalisation.

	NTA	Search FM	Power FM	Crystal FM
Min-Max	0.0384	0.0788	0.1056	0.0963
Decimal Scaling	0.0059	0.0598	0.0349	0.0377
Unitary	0.0123	0.0223	0.0234	0.0218
Z-Score	0.6164	1.3745	1.6838	1.3209

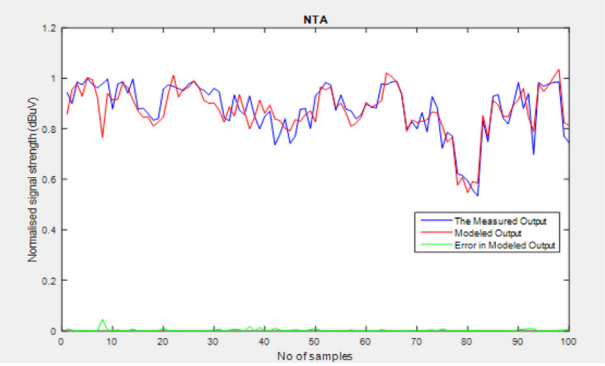

Figure 7. Measured and ANN modeled RSS with MSE for NTA link.

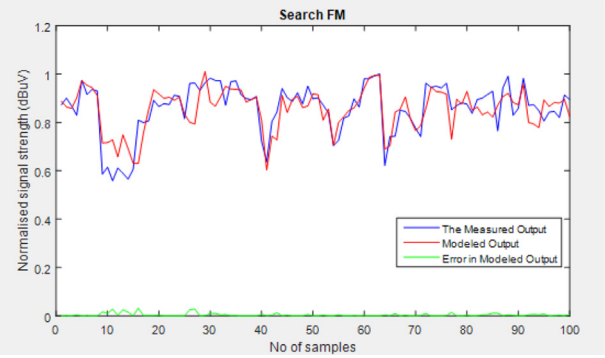

Figure 8. Measured and ANN modeled RSS with MSE for Search FM link.

link using the same ANN derived parameters. The result from the ANN test analysis is presented in Figure 10.

The test analysis carried out as shown in Figure 10 reveal that this model also performed well for the link as modeled signal strength values are reasonably close to the measured signal strength values, and the computed errors are sufficiently low. The computed MSE is 0.0040.

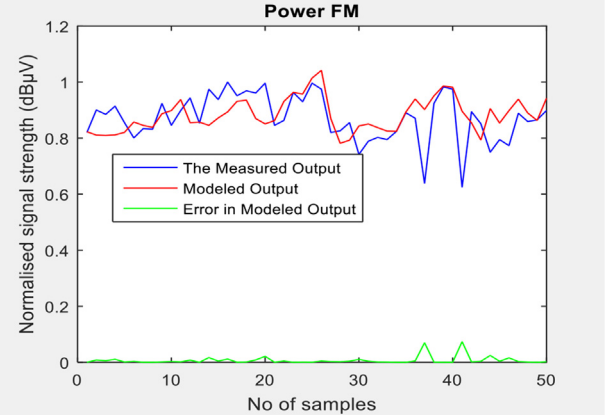

Figure 9. Measured and ANN modeled RSS with MSE for Power FM link.

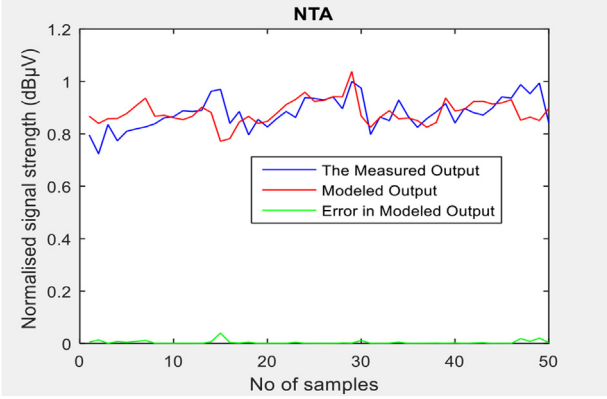

Figure 10. Measured and ANN modeled RSS with MSE for NTA link.

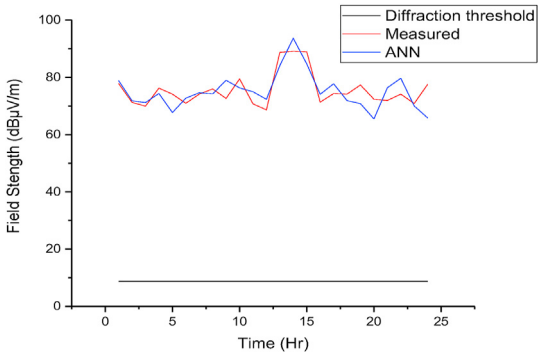

Figure 11. Comparison of measured field strength with ANN and ITU-R models for NTA link.

4.2. Comparison of measured field strength with ANN and diffraction models

The measured signal strength, received as values of voltages were converted to values of electric field strength and was modeled using diffraction

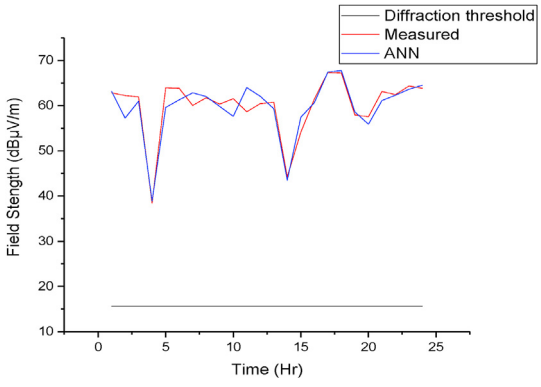

Figure 12. Comparison of measured field strength with ANN and ITU-R models for Search FM link.

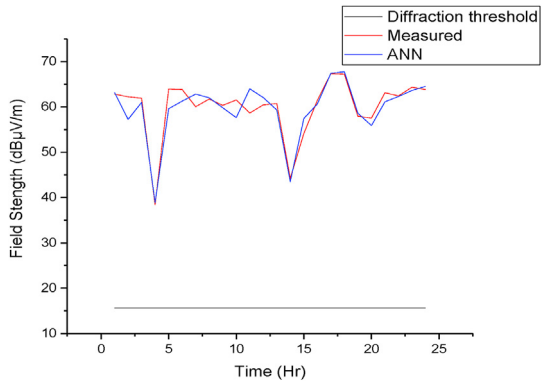

Figure 13. Comparison of measured field strength with ANN and ITU-R models for Crystal FM link.

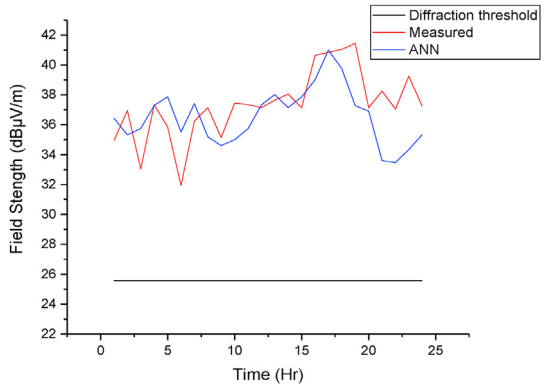

Figure 14. Comparison of measured field strength with ANN and ITU-R models for Power FM link.

formulae according to ITU-R recommendation P. 526. This recommendation uses antenna heights and range to predict path losses due to diffraction over the earth's curvature. Different models that are applicable to different obstacle types and various path geometries are presented in order to evaluate the effect of diffraction on the received field strength. For the links used in this work, a 'smooth terrain' was considered appropriate. Therefore, the prediction model adopted was based on diffraction over spherical earth. The results were compared with measured field strength and the developed ANN models as shown in Figures 11, 12, 13, and 14.

It is observed from Figures 11, 12, 13, and 14 that the ITU-R diffraction model underestimated the received field strength for the four radio links. The differences between the predicted and the measured field strength values are reasonably large. Therefore, there is no correlation between the measured field strength and the ITU-R predicted field strength. For the ANN model, it is clearly seen that computations are very close to the measured field strength data. Hence, good correlation exists between the measured and ANN computed signals except for Power FM link. A correlation coefficient of 0.90 was computed for the NTA link, while that of the Search FM link was 0.50. For the Crystal FM link, the correlation coefficient was 0.87 but the Power FM link had a weak correlation coefficient of 0.20 between the measured and ANN modeled signals.

5. Conclusion

In this work, artificial neural network models that compute VHF signal strength at different frequencies, different transmitting antenna heights and various distances to the receiver using atmospheric parameters have been developed. This was achieved by the application of different types of modeling techniques to the measured signal strength and atmospheric data. Various parameters were evaluated in the training process. These include effects of transfer functions at the hidden and output layers, number of neurons in the hidden layer and data normalisation. The resultant effects of these parameters have been shown to contribute immensely in improving the general performance of the network. In this regard, the combined effects of Tansig transfer function and neuron number 9 in the hidden layer, Purelin transfer function in the output layer and Unitary normalisation yielded the optimal neural network model. The output from the ANN models have shown that the models performed to expectation as computed RSS values were reasonably close to measured RSS values during the training and testing processes. Furthermore, comparing the measured field strength with the ANN and ITU-R P. 526 diffraction models gave good correlation between the measured field strength and the ANN computed signals, but no correlation existed between the measured field strength and the predicted field strength from diffraction model. Hence, it can be concluded that the developed artificial neural network models can compute received VHF signal strength using atmospheric data of temperature, pressure, relative humidity and wind speed in Minna and environs.

Declarations

Author contribution statement

Kingsley Chidozie Igwe: Conceived and designed the experiments; Wrote the paper.

Onyedi David Oyedum: Analyzed and interpreted the data.

Abiodun Musa Aibinu: Performed the experiments.

Michael Oludare Ajewole & Abiodun Stephen Moses: Contributed reagents, materials, analysis tools or data.

Funding statement

This research did not receive any specific grant from funding agencies in the public, commercial, or not-for-profit sectors.

Competing interest statement

The authors declare no conflict of interest.

Additional information

No additional information is available for this paper.

Acknowledgements

The authors appreciate the Center for Atmospheric Research (CAR), Anyigba, which is an activity center of the National Space Research and Development Agency, Nigeria, for providing the equipment used for measuring the atmospheric data.

References

[1] M.V.S.N. Prasad, R.T. Rao, I. Ahmad, K.M. Paul, Investigation of VHF signals in bands I and II in southern India and model comparisons, Indian J. Radio Space Phys. 35 (2006) 198–205.

[2] I. Vilovic, N. Burum, Neural network prediction of signal strength for irregular indoor environments, J. Contr. Meas. Electron. Comput. Commun. Automatika 56 (2015) 55–68.

[3] T.K. Geok, F. Hossain, A.T.W. Chiat, A novel 3D ray launching technique for radio propagation prediction in indoor environments, PloS One 13 (8) (2018), e0201905.

[4] Australian Broadcasting Planning Handbook, Technical Planning Parameters and Methods for Terrestrial Broadcasting, Australian Broadcasting Authority, Canberra, 2004, p. 10.

[5] B.F. Margarita, DSD Variation on Rain Rate Estimate Algorithms of X-Band Polarimetric and Radar and Rainfall Characterization in Tropical Environments Using 2DVD, Rain Gauges and TRMM Data, MSc. thesis, University of Puerto Rico, 2005.

[6] R. Grosskopf, ITU field-strength prediction methods for terrestrial point-to-area services, Proc. of WFMN07, Chemnitz, Germany 2 (B3) (2007) 63–67.

[7] I. Alam, N. Mufti, S.A.A. Shah, M. Yaqoob, The effect of refractivity on propagation at UHF and VHF frequencies, Int. J. Antenn. Propag. 8 (2016) 4138329.

[8] S. Sabu, S. Renimol, D. Abhiram, B. Premlet, A study on the effect of temperature on cellular signal strength quality, IEEE Int. Conf. on Nextgen Electronic Technologies (2017) 38–41.

[9] R. Mat, S.N. Hazmin, R. Umar, S. Ahmad, S.N.A.S. Zafar, M.S. Marhamah, The modelling of tropical weather effects on ultra-high frequency (UHF) radio signals using smartPLS, IOP Conf. Ser. Mater. Sci. Eng. 440 (2018), 012041.

[10] I.R. Gomes, C.R. Gomes, H.S. Gomes, G.P.dS. Cavalcante, Empirical radio propagation model for DTV applied to non-homogenous paths and different climates using machine learning techniques, PloS One 13 (3) (2018), e0194511.

[11] ITU-R, VHF and UHF Propagation Curves for the Frequency Range from 30 MHz to 1000 MHz, Rec. P.370-7, ITU-R P Sers, Int. Telecomm. Union, Geneva, 1995.

[12] ITU-R, Propagation Curves for Aeronautical mobile and Radionavigation Services Using the VHF, UHF and SHF Bands, Rec. P.528-3, ITU-R P Sers, Int. Telecomm. Union, Geneva, 2012a.

[13] ITU-R, Propagation by Diffraction, Rec. P.526-12, ITU-R P Sers, Int. Telecomm. Union, Geneva, 2012b.

[14] ITU-R, Method for point-to-area Predictions for Terrestrial Services in the Frequency Range 30 MHz to 3000 MHz, Rec. P.1546-12, ITU-R P Sers, Int. Telecomm. Union, Geneva, 2012c.

[15] K.C. Igwe, O.D. Oyedum, M.O. Ajewole, A.M. Aibinu, Received signal strength computation for broadcast services using artificial neural network, in: IEEE 13th Int. Conf. On Electronics, Computer and Computation, 2017, pp. 1–6.

[16] J.A. Lane, B.R. Bean, A radio meteorological study, Part I: existing Radio meteorological parameters; Part II: an analysis of V.H.F. field strength variations and refractive index profiles; Part III: a new turbulence parameter, J. Res. Natl. Bur. Std. D67 (1963) 589–604.

[17] D.R. Siddle, E.M. Warrington, S.D. Gunashekar, Signal strength variations at 2 GHz for three sea paths in the British Channel Islands: observations and statistical analysis, Radio Sci. 42 (2007) 1–15.

[18] I. Alam, M. Najam-UI-Islam, U. Mujahid, S.A.A. Shah, R.U. Haq, Refractivity variations and propagation at ultra high frequency, Results in Phys. 7 (2017) 3732–3737.

[19] H. Wennerstrom, F. Hermans, O. Rensfelt, C. Rohner, L. Norden, A long-term study of correlations between meteorological conditions and 802.15.4 link performance, IEEE Int. Conf. on Sensing, Comm. and Netw. (2013) 221–229.

[20] J. Luomala, I. Hakala, Effects of temperature and humidity on radio signal strength in outdoor wireless sensor networks, IEEE Proc. of the Fed. Conf. on Comp. Sci. and Inf. Sys. (2015) 1247–1255.

[21] R. Mat, M.M. Shafie, S. Ahmad, R. Umar, Y.B. Seok, N.H. Sabri, Temperature effect on the tropospheric radio signal strength for UHF band at Terengganu, Malaysia, Int. J. on Advanced Sci. Eng. Inf. Tech. 6 (5) (2016) 770–774.

[22] Y.S. Meng, Y.H. Lee, B.C. Ng, The effects of tropical weather on radio-wave propagation over foliage channel, IEEE Trans. Veh. Technol. 58 (8) (2009) 4023–4030.

[23] ITU-R, Assessment of Impairment Caused to Digital Television Reception by a Wind Turbine, Rec. BT.1893, ITU-R P Sers, Int. Telecomm. Union, Geneva, 2011.

[24] I. Angulo, D. Vega, O. Grande, N. Cau, U. Gil, W. Yiyan, D. Guerra, P. Angueira, Empirical evaluation of the impact of wind turbines on DVB-T reception quality, IEEE Trans. Broadcast. 58 (1) (2012) 1–9.

[25] I. Angulo, D. Vega, I. Cascon, J. Canizo, Y. Wu, D. Guerra, P. Angueira, Impact analysis of wind farms on telecommunication services, Renew. Sustain. Energy Rev. 32 (2014) 84–99.

[26] K. Bronk, A. Lipka, R. Niski, B. Wereszko, Wind farms influence on radiocommunication systems operating in the VHF and UHF bands, TELEKOMUNIKACJA (2015) 44–55.

[27] J.C.F. Pujol, J.M.A. Pinto, A neural network approach to fatigue life prediction, Int. J. Fatig. 33 (2011) 313–322.

[28] J. Schmidhuber, Deep learning in neural networks: an overview, Neural Network. 61 (2015) 85–117.

[29] M. Afrand, A.A. Nadooshan, M. Hassani, H. Yarmand, M. Dahari, Predicting the viscosity of multi-walled carbon nanotubes/water nanofluid by developing an optimal artificial neural network based on experimental data, Int. Commun. Heat Mass Tran. 77 (2016) 49–53.

[30] A.C. Meruelo, D.M. Simpson, S.M. Veres, P.L. Newland, Improved system identification using artificial neural networks and analysis of individual differences in responses of an identified neuron, Neural Network. 75 (2016) 56–65.

[31] G. Dumedah, J.P. Walker, L. Chik, Assessing artificial neural networks and statistical methods for infilling missing soil moisture records, J. Hydrol 515 (2014) 330–344.

[32] S.M. Saad, A.M. Andrew, A.Y. Shakaff, A.R.M. Saad, A.M. Yusof, A. Zakaria, Classifying sources influencing indoor air quality (IAQ) using artificial neural network (ANN), Sensors 15 (2015) 11665–11684.

[33] R.V. Aroca, A.C. Hernandes, D.V. Magalhaes, M. Becker, C.M.P. Vaz, A.G. Calbo, Calibration of passive UHF RFID Tags using neural networks to measure soil moisture, J. Sensors 12 (2018) 3436503.

[34] S. Javeed, K.S. Alimgeer, W. Javed, M. Atif, M. Uddin, A modified artificial neural network based prediction technique for tropospheric radio refractivity, PloS One 13 (3) (2018), e0192069.

[35] H. Zhao, Z. Lai, Neighborhood preserving neural network for fault detection, Neural Network. 109 (2019) 6–18.

[36] A.R. Ozdemir, M. Alkan, M. Kabak, M. Gulsen, M.H. Sazli, The prediction of propagation loss of FM radio station using artificial neural network, J. Electromagn. Anal. Appl. 6 (2014) 358–365.

[37] S. Iliya, E. Goodyear, J. Gow, J. Shell, M. Gongora, Application of artificial neural network and support vector regression in cognitive radio networks for RF power prediction using compact differential evolution algorithm, IEEE Proc. of the Fed. Conf. on Comp. Sci. and Inf. Sys. (2015) 55–56.

[38] J. Isabona, V.M. Srivastava, A neural network based model for signal coverage propagation loss prediction in urban radio communication environment, Int. J. Appl. Eng. Res. 11 (22) (2016) 11002–11008.

[39] B.J. Cavalcanti, G.A. Cavalcante, A hybrid path loss prediction model based on artificial neural networks using empirical models for LTE and LTE-A at 800 MHz and 2600 MHz, J. of Microw., Optoelectronics and Electromag, Appl 16 (3) (2017) 708–722.

[40] J.O. Eichie, O.D. Oyedum, M.O. Ajewole, A.M. Aibinu, Artificial neural network model for the determination of GSM Rxlevel from atmospheric parameters, Eng. Sci. and Tech., an Int. J. 20 (2017) 795–804.

[41] S.I. Popoola, E. Adetiba, A.A. Atayero, N. Faruk, C.T. Calafate, Optimal model for path loss predictions using feed-forward neural networks, Cogent Eng 5 (2018) 1–19.

[42] M.H. Beale, M.T. Hagan, B.D. Howard, Neural Network toolbox™ 7 User Guide, 2011.

[43] G. Zhang, B.E. Patuwo, M.Y. Hu, Forecasting with artificial neural networks: the state of the art, Int. J. Forecast. 14 (1998) 35–62.

[44] A.H. Moghaddam, M.H. Moghaddam, M. Esfandyari, Stock market index prediction using artificial neural network, J. Econ., Fin. and Admin. Sci. 21 (2016) 89–93.